A Novel Fourier-based Approach for Camera Identification

Vittoria Bruni[a], Silvia Marconi[b] and Domenico Vitulano[c]
Department of Basic and Applied Sciences for Engineering, Sapienza Rome University, via Antonio Scarpa 14-16, 00161 Rome, Italy

Keywords: Camera Identification, PRNU, Fourier Transform.

Abstract: In this paper the source camera identification problem is considered and novel features for PRNU noise are studied. The regularity of a suitable sampling of the PRNU image is considered and it is measured through the decay of its Fourier spectrum. This single global feature is independent of image filtering and size, but it carries significant information concerning the image. The aim is to use this feature in the classification step. Some preliminary results show that this kind of approach is promising as it is able to reach identification scores that can be comparable to the reference source camera identification method, without requiring any image downsampling or cropping.

1 INTRODUCTION

The increasing use of images and videos in several multimedia applications has offered new research challenges and problems. One of the most interesting is Image Forensic, due to the crucial role of images and videos for several investigation purposes, such as identification of the sources that took images, authenticity, robustness of data transmission, storage and manipulation — just to cite a few. Among the aforementioned problems, probably the most fascinating is camera identification (Al-Ani and Khelifi, 2017; Lukas et al., 2006) as having several implications in forensics (Chen et al., 2008; Chierchia et al., 2010; Korus and Huang, 2016). Coarsely speaking, it mainly consists of looking for a reliable correspondence between a given image and the device that took it. One of the most adopted (and powerful) tools for camera identification is PRNU (Photo Response Non Uniformity noise). It consists of a noise component in any acquired image that is caused by the CCD imperfections, so that particular pixels are susceptible to giving brighter intensities than others. This peculiarity plays a crucial role as it is a sort of fingerprint of the device that in principle makes it easy to recognize. Unfortunately, this is not the case as it is very difficult to extract PRNU from a given image. That is why a plethora of approaches has been proposed in the last years concerning this topic.

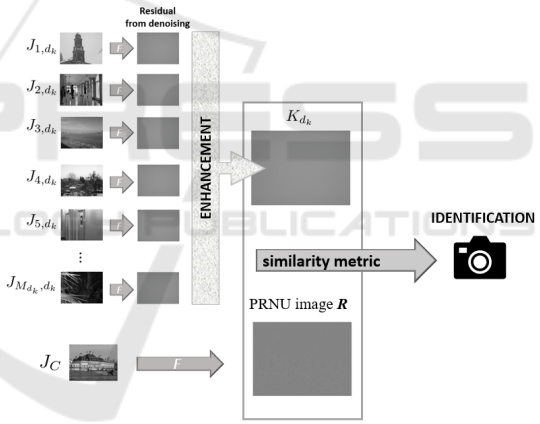

Figure 1: Block scheme of the whole pipeline for camera identification problem.

Coarsely speaking, camera identification problem can be seen from two different points of view: forensic and scientific. Keeping in mind forensics requirements, it is possible to give a coarse taxonomy of the proposed approaches (Caldelli et al., 2018; Chierchia et al., 2014; Korus and Huang, 2016; Marra et al., 2017; Valsesia et al., 2017) by considering the most frequent cases, briefly described below:

1. given a set of available devices and an image acquired by one of them, the goal consists of looking for which device took the image;

[a] https://orcid.org/0000-0003-3909-7463
[b] https://orcid.org/0000-0002-4916-4896
[c] https://orcid.org/0000-0001-6088-9743

Bruni, V., Marconi, S. and Vitulano, D.
A Novel Fourier-based Approach for Camera Identification.
DOI: 10.5220/0010437000990106
In *Proceedings of the International Conference on Image Processing and Vision Engineering (IMPROVE 2021)*, pages 99-106
ISBN: 978-989-758-511-1

2. given a set of available devices and an image, the goal consists of determining whether the device taking that image belongs to such a set;
3. given a set of images, the goal is to group them according to the corresponding source.

Sometimes, the requirements above can be relaxed and it may be sufficient to solve subproblems such as to find out only the brand or the model - rather than the specific device. From a scientific/practical point of view, the problems above necessarily require two main steps: PRNU extraction and PRNU comparison (via a suitable metric). With regard to PRNU extraction, several approaches adopt denoising techniques that allow to get the noise (i.e., PRNU) in terms of the residual image. PRNU comparison represents an even more difficult task because of PRNU noisy nature — for approaches belonging to this class that mainly focus on clustering, see for instance (Georgievska et al., 2017; Huang et al., 2015; Marra et al., 2017). To further complicate the problem, distortions introduced by image upload/download from the social networks have to be accounted for, as they often represent the actual available data (Caldelli et al., 2018; Valsesia et al., 2017). Fig. 1 depicts the whole source camera identification pipeline. It is evident that each block in the pipeline gives a contribution to the final result in terms of error. For instance, PRNU extraction usually employs a classical denoising process — as in the pioneering work of Lukas et al. (Lukas et al., 2006). Since denoising is not perfect, as a side effect one achieves a mix of PRNU and image components that usually alters the final result. Even though different and more sophisticated approaches have been proposed in the literature (Akshatha et al., 2016; Al-Ani and Khelifi, 2017; Salvi and Vitulano, 2019; Fridrich, 2009; Tiwari and Gupta, 2018; Kumar and Hassebrook, 1990; Li et al., 2018; Thaia et al., 2015; Xu et al., 2016; Zhao et al., 2019), the problem still holds. On the other hand, PRNU comparison is delicate due to the impulsive (and quasi random) nature of PRNU. It is straightforward that in the camera identification problem a cumulative error occurs and it is difficult to separate and quantify the contribution of each specific phase.

In this paper we step back to reformulate the problem as the following subproblem. Specifically, we work on flat fields images, i.e. those representing a uniform and flat background — thus mainly containing PRNU. This assumption, although simplistic, allows us to by-pass all problems due to network uploading/downloading and PRNU extraction. The (sub)problem we aim to address is: which is the best way to represent and compare two PRNUs? Although simpler, it remains a hard problem because two noisy signals have to be compared. If they have no distortion, the correlation method proposed in (Lukas et al., 2006) is very performing. Unfortunately, this is not the real case in practice. Hence, the question is now if it is possible to differently represent PRNU in order to use classical image processing tools to get better results. To this aim, a different PRNU representation is proposed. It consists of suitably rearranging it in order to increase its visual regularity. A simple example is shown in Fig. 2. The interesting aspect of this approach is twofold. On the one hand, the resulting image is more intellegible from a visual point of view; on the other hand, this image is more "tractable" by means of classical signal processing tools. In particular, the decay of the Fourier spectrum is considered as representative of the global signal regularity, and it has been used as single feature in the source identification process, as described in the first case of forensics requirements listed at the beginning of this section. Even if this is a first attempt to give a different representation of a PRNU signal, to the best of the authors knowledge, it has various advantages: *i)* it reaches comparable performance to the classical correlation approach in (Lukas et al., 2006) when comparing images having the same size, even if just one global spectrum parameter rather than the whole PRNU image is employed; *ii)* it is independent of the image size so that no resinzing or cropping is required for comparing device PRNU and image PRNU (more realistic scenario).

Preliminary results have been achieved on the publicly available Dresden database (Gloe and Bhme, 2010) and identification results have been studied in different conditions. Particular attention has been devoted to the ability of the single global feature to correctly assign each image to the corresponding device; as it will be shown, the estimation of this parameter on different regions of the image allows us to define an array of features that contributes to further increase identification performance.

The remainder of the paper is the following. Next section presents the proposed method along with some theoretical and practical motivations. Section 3 presents some preliminary experimental results, while the last section draws the conclusions.

2 THE PROPOSED MODEL

In the literature, the observed image is modelled as

$$J(x,y) = I(x,y) + I(x,y)K(x,y) + N(x,y),$$

where J is the acquired image, (x,y) the pixel location, I is the original image content, K is the PRNU

Figure 2: Two different PRNU representations: Top: Conventional PRNU matrix, Bottom: PRNU matrix whose values have been sorted row-wise and then column-wise.

component while N represents other noise sources that are independent of K (Lukas et al., 2006). K is a zero-mean noise component that is independent of I and it is specific for the device that took the image J.

As it can be observed, the original image plays a crucial role in the equation above and then the extraction of K is a very delicate operation and active research field. However, if an almost constant image is acquired, we get a flat field (FF) image that can be briefly written as

$$J(x,y) = B + BK(x,y) + N(x,y),$$

where B denotes the constant background. Despite the presence of the noise component N, FF image better reveals K. That is why, whenever possible, flat field images are used for estimating device PRNU, i.e. the reference pattern. The common procedure for K estimation is described below and it also characterizes the most famous and pioneering approach for source camera identification presented in (Lukas et al., 2006).

A set of m images having almost constant background is acquired, i.e.

$$J_i(x,y) = B_i + B_iK_i(x,y) + N_i(x,y), \quad i = 1,..,m;$$

a denoiser F is applied to each J_i and the residual image is extracted, i.e. $R_i = J_i - F(J_i)$. Since the images J_i, $i = 1,...,m$ have been acquired by the same device and the noise sources N_i are iid, then K can be estimated either as a simple pixelwise mean of the estimated residuals R_i or through the maximum likelihood estimator, i.e. $K = \frac{\sum_{i=1}^{m} R_i J_i}{\sum_{i=1}^{m} J_i^2}$. The latter method is more robust and it allows for a more accurate estimation of the reference pattern.

The same denoising procedure is applied whenever the PRNU from a single image has to be extracted. In order to assess if an image W has been taken by a given device, the normalized correlation between the estimated reference pattern K and the residual R for the image W is computed, i.e. $\rho(K,R) = \frac{\sigma_{KR}}{\sigma_K \sigma_R}$, where σ_{KR} is the cross correlation between K and R, while σ_K and σ_R are the standard deviations of K and R respectively. The closer to 1 ρ, the higher and more reliable the match between the image W and the device having K as reference pattern.

Even though this kind of approach provides satisfying results, the use of correlation implies a perfect match between K and R dimension; if it is not the case, some resizing/cropping is required but this would cause the modification of noise component or misalignments between the comparing noise components. In addition, correlation values are in general close to zero as the denoising process cannot perfectly separate PRNU from the remaining noise sources. Finally, the accuracy of correlation decreases whenever the original image has been altered by some operations, as for example, the upload or download from the web or social networks. That is why in this paper we are interested in contributing to solve the first problem. i.e. to find novel features for K image that can be used independently of the image size. For the same reason, flat fields images will be analysed.

The decreasing/increasing rearrangement is a well known concept in mathematics (Duff, 1967) but it is also used in signal processing as rank ordering for continuous-time signals (Ferreira, 2001). It consists of a sorted version of the original signal. In a more formal setting, the decreasing rearrangment f^* of f is defined as the inverse of the cumulative distribution of the function f. As a result, f^* is a function having some nice properties and relations with the original one; more precisely, it preserves some interesting properties of f, such as mean, energy, distribution function and global regularity — see (Duff, 1967; Ferreira, 2001) for details. In the studied case, the function f is the image K and we are interested in studying and exploiting the properties of its sorted counterpart K^*. In particular, we empirically observed that K^*, that has been defined by rearranging the values of K in increasing order along the x (rows) and y (columns) direction, shows some geometrical structures that seem to characterize the single device. An example is shown in Fig. 3, where K^* of distinct devices are depicted. As it can be observed, these sorted images present a peculiar pattern that allows for discriminating between different de-

Figure 3: Top: Device. Bottom: corresponding rearranged PRNU matrix K^* for three different devices belonging to three different brands.

vices. In fact, for each considered device, a different pattern is observable, while for the same device, the same pattern is provided by distinct flat field images, as Fig. 4 shows. We then conclude that the characterization of the observed pattern enables the characterization of the device and, in particular, it can contribute to discriminating images acquired by different devices. This observation motivates our work whose aim is then to define features for the observed behaviour.

In particular, if we design an ideal straight line from the topleft corner to the bottommost right one, i.e. the diagonal of the rectangular image domain, we get a signal that captures most of the observed geometrical structure, as Fig. 5 shows. Hence, the aim

Figure 4: Rearranged flat field images acquired by the same device. The first device in Fig. 3 has been considered.

is to provide a feature of the resulting signal and to evaluate to what extent it is able to represent/identify the whole reference PRNU. To this aim we made the following observations:

- the geometrical patterns are mainly characterized by a different frequency of the repeated structures (sort of pseudospherical waves having specific wavelength). We then expect that this kind of feature is mainly emphasized and measurable in the signal spectral components;
- one of the main feature of a function is its regularity that can be measured through its global Lipschitz exponent;
- the decay of the Fourier spectrum is stricly correlated to signal global Lipschitz exponent.

It turns out that the decay of the modulus of the coefficient of the Fourier transform of the diagonal of the rank sorted matrix K^* of the PRNU image is the feature that is worth to investigate. In the sequel $f(y)$ will identify the intensity signal corresponding to the diagonal of the rectangular K^* domain.

2.1 Fourier Spectrum Decay as PRNU Feature

One of the main features of a function is its regularity. The latter can be referred to the whole function, i.e.

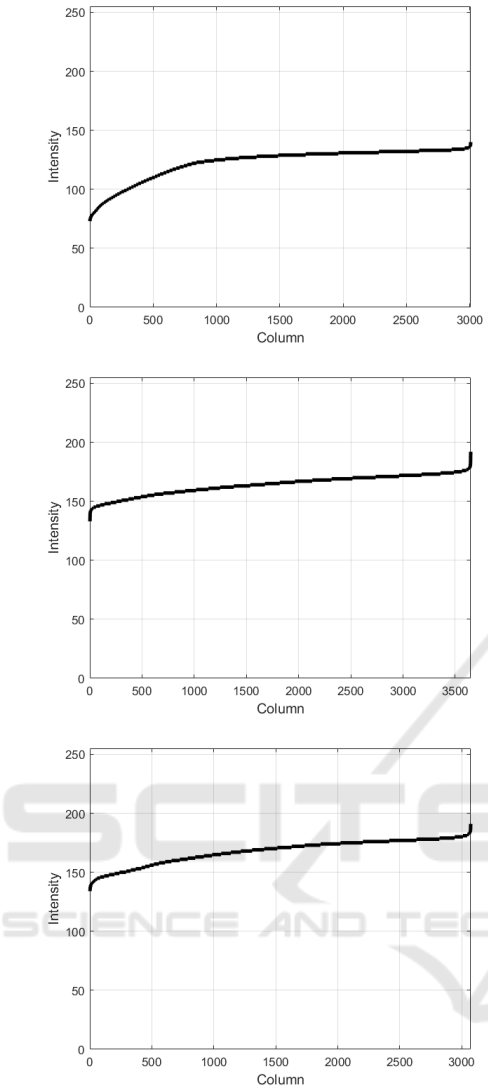

Figure 5: Intensity signal corresponding to the diagonal of the rectangular domain of K^*. Plots are referred to the blue color channel of the images depicted in Fig. 3.

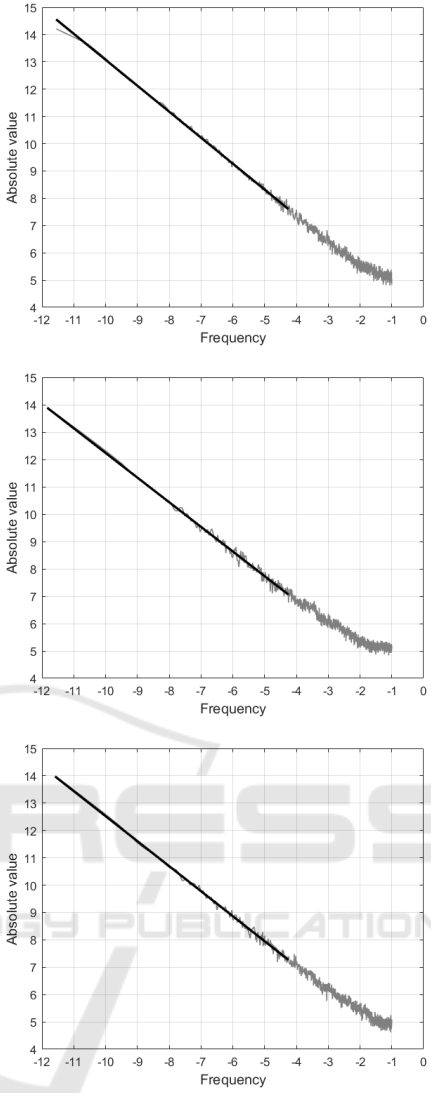

Figure 6: Loglog plot of the Fourier spectrum of the Intensity signals in Fig. 5 (gray line). The estimated straight line, as in eq. (3), using the first 10% frequencies, except for the DC term, is also depicted (black line).

global regularity, or it can be considered locally (local regularity). Independently of its kind, regularity can be measured as the Lipschitz regularity (Mallat, 1998). We recall that a function f is uniformly Lipschitz over an interval $[a,b]$ of the real axis if for each $y \in [a,b]$ there exist a positive constant C independent of y and a polynomial p_y of degree $\lfloor \alpha \rfloor$ such that

$$\forall\, v \in [a,b] \quad |f(v) - p(v)| \leq C|y-v|^{\alpha}. \qquad (1)$$

If $\alpha < 1$, then α characterizes the singularity type. Furthermore, if $f(y)$ is the signal under study, $\hat{f}(\omega)$ its Fourier transform, ω the frequency, and if

$$|\hat{f}(\omega)| \leq \frac{C}{1+\omega^{1+q+\delta}}, \qquad (2)$$

with C and δ two positive constants, then f is smooth and q is the order of smoothness. The same result holds whenever the smoothness is measured in terms of Lipschitz exponent α. As a result, by measuring the asymptotic decay of the modulus of the Fourier transform of the signal f, we get some information concerning its global regularity.

Based on these results, we consider the global Lipschitz exponent α of f and, without loss of generality, we relax the relation in eq. (2) as $|\hat{f}(\omega)| \leq \frac{C}{|\omega|^{1+\alpha+\delta}}$. By taking the logarithm to both members, we get

$$log(|\hat{f}(\omega)|) \leq log(C) - (1+\alpha+\delta)log(|\omega|) \qquad (3)$$

so that α regulates the slope of a straight line that

bounds the logarithm of the absolute value of the Fourier transform. Hence, a least squares regression on $log(|\hat{f}(\omega)|)$ allows for the estimation of the slope of the straight line, and then α — see Fig. 6.

It is worth observing that the regularity measured in the sorted signal is not independent of the regularity of the original signal so that the estimated regularity is strictly related, in some sense, to the regularity of the original PRNU (Ferreira, 2001). This observation further motivates the choice of focusing on the properties of the rank sorted matrix. On the other hand, α is a global feature, but eq. (1) also holds locally. Hence, in order to better characterize the analyzed PRNU image, the same Lipschitz exponent estimation procedure can be applied on subregions of the whole image. In this way a more local information is embedded in the estimated Lipschitz coefficients and a vector of features can be defined for the image under study. The components of this features vector are the Lipschitz coefficients estimated on each image subregion Ω_j, $j = 1, ..., M$. In this paper, rectangular subregions have been considered by partitioning the image into sub-blocks having the same size.

2.2 The Algorithm

Before presenting the proposed source identification algorithm in details, it is worth observing that, each color channel can be processed separately and the coefficients estimated for each color channel, respectively $\alpha_R, \alpha_G, \alpha_B$, define the feature vector associated to PRNU image. The second observation is the following. K regularity can be estimated directly from flat field images by excluding the highest spectrum frequencies, where the contribution of the noise component N cannot be considered negligible. In this way we do not need to estimate the reference pattern K for each device, but the corresponding features vector can be directly estimated as

$$\alpha_R = \frac{1}{m}\sum_{i=1}^{m}\alpha_{R,i},\ \alpha_G = \frac{1}{m}\sum_{i=1}^{m}\alpha_{G,i},\ \alpha_B = \frac{1}{m}\sum_{i=1}^{m}\alpha_{B,i}, \tag{4}$$

where $\alpha_{*,i}$ is the Lipschitz exponent of the * color channel of the flat field image J_i. In other words, for each color channel, the average of the regularity coefficients estimated from each flat field image acquired by the same device is considered. As a result, it is not necessary to adopt any denoising or averaging method for K estimation.

The source identification algorithm is then sketched as below.

Let W be the image to be classified and let $J_{i,d}$, $i = 1, ..., m$ the set of FF images acquired by the d-th device.

1. For each device d
   - compute the feature vector $\alpha_i = (\alpha_{R,i}, \alpha_{G,i}, \alpha_{B,i})$ for each flat field image $J_{i,d}$ by linear regression according to eq. (3), where f is the diagonal of $J^*_{i,d}$ domain
   - set $\alpha_d = (\alpha_R, \alpha_G, \alpha_B)$, with α_* computed as in eq. (4). α_d is the reference feature vector for the device d
2. Compute the feature vector α for the image W
3. For each device d, compute the distance $\mathcal{D}$ between α and α_d, i.e.
$$\mathcal{D}(\alpha, \alpha_d) = \|\alpha - \alpha_d\|_2$$
4. Assign the image W to the device $\bar{d}$ realizing the minimum distance value, i.e.
$$\bar{d} = argmin_d \mathcal{D}(\alpha, \alpha_d).$$

3 EXPERIMENTAL RESULTS

The proposed feature has been tested on the publicly available Dresden database (Gloe and Bhme, 2010) that includes hundred images (natural and flat field) captured by several camera models and devices. For comparative studies, the method in (Lukas et al., 2006) has been considered as the reference pioneering one. The objective of the presented tests is to quantify the ability of the proposed (single) feature in assigning each image in the database to its source device. In all tests W is a flat field image and all the flat field images in the database have been considered in the source identification task. Hence, if $W = J_{i,d}$, with fixed i, is the image to be classified, then it is compared with all the devices in the database but the feature vector for the device d, i.e. α_d, is estimated using all the flat field images taken by d except for the one assigned to W. In addition, the range of frequencies used for Fourier spectrum decay has been empirically set equal to 10% of the whole spectrum range.

Table 1 refers to results achieved on the whole dataset, where the success rate is provided. The latter is measured as the percentage of correct assignments with respect to the number of considered candidate images. As it can be observed, the success rate of the proposed method is not negligible, especially if one takes into account that just one global image feature (one parameter for each color channel) has been used in the matching phase. In fact, one of the main advantage of the proposed approach is the use of a single and easy to compute image feature in the identification process; the adopted feature is independent of image size and spatial correspondences between the two comparing images.

Table 1: Success rate provided by the proposed method on Dresden database (*first column*) and the ones provided by the same method applied to the images partitioned into M equally size subblocks.

	Proposed	Proposed ($M = 4$)	Proposed ($M = 16$)
Device	51.4	85.3	92.8
Model	64.6	92.9	96.9
Brand	67.2	94.7	98.1

In order to further evaluate the advantages and/or limits of the proposed method, brand and model classification rates have also been considered. As it can be observed in the same table, the success rate increases as the reference set enlarges. This means that many of the incorrect device assignments are within the same device model or, more in general, within the same device brand. As a result, the proposed feature is able to capture the characteristics of the "device family".

Table 1 also contains the results achieved by the proposed method whenever images are partioned in 4 and 16, respectively, rectangular subregions having the same size and the vector of coefficients estimated in each subregion is used for classification purposes. This application mode allows for better capturing some local image features. As it can be observed, identification success rate significantly increases thanks to the use of a more local information.

In order to perform comparative studies, the proposed method using 16 sub-blocks has been considered and two different subsets of devices have been extracted from Dresden database. The first testing set is composed of 23 devices (belonging to 7 brands) whose flat field images have the same size (see Table 2); the total number of images in this set is 950. The second testing set is composed of 21 devices (belonging to 8 brands) whose flat field images can have different dimension (see Table 3); the number of images in the whole subset is 900. For the second testing set, the method in (Lukas et al., 2006) requires cropping or subsampling in order to compare the normalized correlation coefficient. As Table 4 shows, although the use of a single global feature, the proposed method allows to reach moderately high success rates. Even in this case, the success rate increases whenever model and brand assignments are considered. The same table contains the results achieved by the reference method in (Lukas et al., 2006) whenever the denoising step is omitted in the estimation of device reference PRNU. In this way the two methods have comparable computational complexity. As it can be observed, the proposed method achieves results that are close to the basic version of the method in (Lukas et al., 2006), i.e. 100%, but it outperforms it whenever denoising is not applied. These results prove a certain robustness of the proposed feature to background noise.

Table 2: Testing set I: the images have the same size, i.e. 2736×3648. For each model, the number of devices and the number of images for each device is provided.

Model	no. Devices	no. Images
Olympus MJU	5	50
Pentax Optio A40	1	50
Samsung NV15	3	50
Sony Cyber-shot DSC-T77	4	50
Sony Cyber-shot DSC-W170	2	50
Panasonic Lumix DMC-FZ50	2	25
Ricoh Caplio GX100	5	25

Table 3: Testing set II: the images have different size.

Model	Image size	no. Dev.	no. Imgs
CanonIXUS55	1944×2592	1	50
CanonIXUS70	2304×3072	3	50
NikonS710	3264×4352	5	50
NikonD200	2592×3872	2	25
NikonD70	2000×3008	2	25
NikonD70S	2000×3008	2	25
SamsungL74	2304×3072	3	50
SamsungNV15	2736×3648	3	50

4 CONCLUSIONS

In this paper a novel feature for PRNU image has been proposed and its contribution to source camera identification has been evaluated. It consists of the decay of the Fourier spectrum of a particular sampling of a sorted version of PRNU matrix. This decay is strictly related to the regularity of the signal under study and then it represents one of its representative features. As the paper presented a feasibility study, flat field im-

Table 4: Success rate on two different testing sets: comparisons between the proposed method (Prop.) using image partitioning into 16 subblocks and the method (Lukas et al., 2006) (**L06**) when denoising filter is not applied before FF averaging in the estimation of the reference pattern.

	Testing set I		Testing set II	
	Prop.	**L06**	Prop.	**L06**
Device	99.5	99,2	92.9	94.7
Model	99.9	99.9	92.9	99.9
Brand	99.9	99.9	92.9	99.9

ages have been considered. Preliminary and extensive tests performed on a publicly available database have shown that the proposed feature has some potential in contributing to the solution of the source identification problem and it is able to reach high success rates whenever properly estimated. On the other hand, it has the advantage of being independent of image size, so that artificial operations are useless whenever two PRNU images have to be compared; finally, due to its nature, it can show some robustness to background noise sources. Future research will be then devoted to refine the proposed feature, making it able to capture both global and local image characteristics; to extend it to natural images and to evaluate its performance on natural images and different datasets.

REFERENCES

Akshatha, K., A.K. Karunakar, H. A., Raghavendra, U., and Shetty, D. (2016). Digital camera identification using prnu: A feature based approach, digital investigation. In *Digital Investigation*.

Al-Ani, M. and Khelifi, F. (2017). On the spn estimation in image forensics: A systematic empirical evaluation. In *IEEE Trans. on Inf. Forensics and Security*.

Caldelli, R., Amerini, I., and Tsun, L. C. (2018). Prnu-based image classification of origin social network with cnn. In *Proc. of EUSIPCO 2018*.

Chen, M., Fridrich, J., Goljan, M., and Lukas, J. (2008). Determining image origin and integrity using sensor noise. In *IEEE Trans. on Inf. Forensics and Security*.

Chierchia, G., Parrilli, S., Poggi, G., Sansone, C., and Verdoliva, L. (2010). On the influence of denoising in prnu based forgery detection. In *Proc. of the 2nd ACM workshop on Multimedia in forensics, security and intelligence*.

Chierchia, G., Poggi, G., Sansone, C., and Verdoliva, L. (2014). A bayesian-mrf approach for prnu-based image forgery detection. In *IEEE Trans. on Information Forensics and Security*.

Duff, G. F. D. (1967). Differences, derivatives, and decreasing rearrangements. In *Canadian Journal of Mathematics*.

Ferreira, P. (2001). Sorting continuous-time signals: Analog median and median-type filters. In *IEEE Trans. on Signal Processing*.

Fridrich, J. (2009). Digital image forensics. In *IEEE Signal Processing Magazine*.

Georgievska, S., Bakhshi, R., Gavai, A., Sclocco, A., and van Werkhoven, B. (2017). Clustering image noise patterns by embedding and visualization for common source camera detection. In *Digital Investigation*.

Gloe, T. and Bhme, R. (2010). The dresden image database for benchmarking digital image forensics. In *Journal of Digital Forensic Practice*.

Huang, Y., Zhang, J., and Huang, H. (2015). Camera model identification with unknown models. In *IEEE Trans. on Information Forensics and Security*.

Korus, P. and Huang, J. (2016). Multi-scale analysis strategies in prnu-based tampering localization. In *IEEE Trans. on Information Forensics and Security*.

Kumar, B. V. K. V. and Hassebrook, L. (1990). Performance measures for correlation filters. In *Appl. Opt.*

Li, R., Li, C. T., and Guan, Y. (2018). Inference of a compact representation of sensor fingerprint for source camera identification. In *Pattern Recognition*.

Lukas, J., Fridrich, J., and Goljan, M. (2006). Digital camera identification from sensor pattern noise. In *IEEE Trans. on Information Forensics and Security*.

Mallat, S. (1998). A wavelet tour of signal processing. In *Academic Press*.

Marra, F., Poggi, G., Sansone, C., and Verdoliva, L. (2017). Blind prnu-based image clustering for source identification. In *IEEE Trans. on Inf. For. and Sec.*

Salvi, V. B. A. and Vitulano, D. (2019). Joint correlation measurements for prnu-based source identification. In *Lecture Notes in Computer Science, (Proc. of CAIP 2019)*.

Thaia, T. H., Retraintband, F., and Cogranne, R. (2015). Camera model identification based on the generalized noise model in natural images. In *Digital Signal Processing*.

Tiwari, M. and Gupta, B. (2018). Efficient prnu extraction using joint edge-preserving filtering for source camera identification and verification. In *Proc. of IEEE ASPCON 2018*.

Valsesia, D., Coluccia, G., Bianchi, T., and Magli, E. (2017). User authentication via prnu-based physical unclonable functions. In *IEEE Trans. on Information Forensics and Security*.

Xu, B., Wang, X., Zhou, X., Xi, J., and Wang, S. (2016). Source camera identification from image texture features. In *Neurocomputing*.

Zhao, Y., Zheng, N., and T. Qiao, M. X. (2019). Source camera identification via low dimensional prnu features. In *Multimedia Tools and Applications*.